Wireless Personal Communications **21:** 5–28, 2002.

Closed-Form Estimators for Blind Separation of Sources – Part I: Real Mixtures

VICENTE ZARZOSO* and ASOKE K. NANDI
Signal Processing and Communications Group, Department of Electrical Engineering and Electronics, The University of Liverpool, Brownlow Hill, Liverpool L69 3GJ, U.K.
E-mail: vicente@liverpool.ac.uk

Abstract. The problem of multiuser interference cancellation in wireless cellular communication systems accepts a blind source separation (BSS) model. The present contribution studies the closed-form solutions to BSS in the real-mixture case. Connections among a number of seemingly disparate methods are unveiled, new procedures are put forward, and their asymptotic (large-sample) performance is analyzed. Simulation experiments illustrate and validate the theoretical results. Altogether, a unifying generic framework for closed-form BSS methods is developed.

Keywords: blind source separation, closed-form estimators, contrast functions, higher-order statistics, independent component analysis, multiuser detection, performance analysis.

1. Introduction

1.1. Problem and Motivation

Traditional non-interfering (in time or frequency) multiple access schemes (TDMA, FDMA) cannot cope with the rising demands for increased capacity, faster data rates, and higher quality and flexibility of services in digital mobile networks. By contrast, interfering multiaccess techniques – such as code division multiple access (CDMA) – allow a trade-off between reception quality and increased capacity ("soft capacity"), making the sharing of channel resources inherently dynamic and considerably more efficient than with conventional multiaccess procedures [25, 26]. Additional features such as "soft handover", asynchronism, and re-utilization of the entire bandwidth in every cell (reuse factor of one) have transformed (wideband) CDMA into the strongest candidate for the third generation wireless personal communication systems [19, 25].

The performance of CDMA systems is limited by the interference caused by active users within the same cell (multiuser interference, MUI). Substantial capacity gains may be achieved by appropriate suppression of MUI, especially when capitalizing on the interference structure, giving rise to the design of multiuser detection (MUD) techniques [25, 26] in the physical layer of the wireless system. MUD consists of the separation of the users' transmitted signals that appear mixed at the receiving antenna output. If an antenna array is available (as may in the uplink), spactial diversity can be exploited; otherwise (as is more likely in the downlink), diversity may be provided by the users' orthogonal signature waveforms [25].

* Supported through a Post-doctoral Research Fellowship awarded by the Royal Academy of Engineering, U.K.

In the general case, a set of stochastic processes $\boldsymbol{y} = [y_1, \ldots, y_p]^{\mathrm{T}} \in \mathbb{C}^p$ (symbol $^{\mathrm{T}}$ denotes the transpose operator) are observed at the output of a p-dimensional sensor (perhaps virtual, if no spatial diversity is available). Each of the received signals can be considered as an unknown mixture of the unobservable q transmitted *source signals* $\boldsymbol{x} = [x_1, \ldots, x_q]^{\mathrm{T}} \in \mathbb{C}^q$ which may be assumed statistically independent. The effects of frequency-selective multipath propagation amount to (time-varying) linear filtering of the transmitted signals, resulting in a convolutive mixture at the receiving end. In the cases where multipath effects can be neglected – as in flat-fading environments – the mixture becomes instantaneous, and follows the matrix model:

$$\boldsymbol{y} = \boldsymbol{M}\boldsymbol{x} + \boldsymbol{n}\,. \tag{1}$$

Matrix $\boldsymbol{M} \in \mathbb{C}^{p\times q}$ represents the mixing structure – determined by the transmitter-receiver relative positions, users' codes, propagation conditions, etc. – and vector $\boldsymbol{n} \in \mathbb{C}^p$ accounts for possible additive sensor noise. The MUD problem reduces to recovering the source data vector $\boldsymbol{x}$ from the sensor output $\boldsymbol{y}$.

Conventional beamforming techniques parameterize the mixing matrix $\boldsymbol{M}$ in terms of the array structure. However, the array manifold is often unknown or difficult to model, causing calibration errors which hinder the source extraction. In this respect, operating blindly, i.e., assuming no particular structure for $\boldsymbol{M}$, benefits from a more robust performance [4]. Equation (1) then corresponds to the blind source separation (BSS) model in instantaneous linear mixtures [31]. The separation is accomplished by maximizing, explicitly or otherwise, the degree of statistical independence between the output components, a process known as independent component analysis (ICA) [7].

Typically, no assumptions can be made about the noise, so one may concentrate on solving the noiseless BSS problem. The conventional may be adopted that the sources are unit power, since a scalar factor can be interchanged between each source and its corresponding column of the mixing matrix without altering the observations. This is one of the basic BSS indeterminacies. The other is related to the ordering of the sources, which is obviously irrelevant unless some prior information is available. If the time structure of the observed signals is ignored or cannot be exploited (as in the i.i.d. case) the source separation can only be accomplished through the application of higher-order statistics (HOS).

1.2. Other Applications of BSS

Motivated by the vast amount of potential applications and the increasing interest in the area of HOS, the BSS problem has received a great deal of attention during the last decade. Indeed, there are a great number of situations in which one desires to recover unobservable signals from measurements of their mixtures. Along with wireless communications and array signal processing, the area of biomedical signal processing has greatly benefited from the application of BSS techniques [13]. Problems such as the extraction of brain electric activity sources from the electroencephalogram (EEG), as well as the removal of artifacts in EEG recordings, can be successfully tackled by means of ICA [17]. The non-invasive extraction of fetal heartbeat signals from maternal electrocardiogram (ECG) recordings – corrupted by the strong maternal heartbeat components and other sources of interference – can also be neatly carried out via BSS [16], which is shown to outperform conventional techniques [35]. More recently [20], BSS has arisen as a novel, promising technique for the extraction of atrial activity in episodes of atrial fibrillation, a common cardiac arrhythmia. Other interesting applications include speech/audio processing [24] and seismic exploration [23].

1.3. BSS Problem after Pre-Whitening

Second-order processing – e.g., eigen-decomposition or principal component analysis (PCA) of the sensor-output covariance matrix – results in a set of normalized uncorrelated signals, $\boldsymbol{z} = [z_1, \ldots, z_q]^T \in \mathbb{C}^q$, which are referred to as whitened signals. They are related to the true sources through a unitary transformation [5, 10, 30, 31]:

$$\boldsymbol{z} = \boldsymbol{Q}\boldsymbol{x} \,. \tag{2}$$

Therefore, the source separation reduces to the estimation of matrix $\boldsymbol{Q}$. If $\widehat{\boldsymbol{Q}}$ is a correct estimate of such matrix, then the output

$$\boldsymbol{s} = \widehat{\boldsymbol{Q}}^{-1}\boldsymbol{z} = \widehat{\boldsymbol{Q}}^{\mathrm{H}}\boldsymbol{z} \tag{3}$$

($^{\mathrm{H}}$ being the conjugate-transpose operator) recovers the sources up to the scale and ordering indeterminacies cited at the end of Section 1.1

1.4. Closed-Form Solutions

A great variety of different approaches have been proposed in the literature over the last few years [4, 3, 7, 18], but our focus is on those whereby unitary matrix $\boldsymbol{Q}$ (or, rather, the parameter(s) it depends on) is estimated in analytic or closed-form, as opposed to techniques requiring iterative optimization (e.g., [15]) or other computationally demanding procedures. The main attribute of closed-form solutions is their simplicity and mathematical tractability. Essentially, closed-form methods obtain parameter estimates directly by means of a formula composed of certain whitened-vector statistics. Specific methods differ in the statistics and formulae used. It is shown in [5] that this direct estimation is indeed possible in the two-source two-sensor case, and an analytic solution is found by nulling the output cross-cumulants at order 4. This solution is extended to the complex case in [6]. The maximum-likelihood (ML) principle together with extra assumptions on the source distribution yields another 4th-order closed-form estimator [10]. These constraints are actually too restrictive: a similar expression is found through a rather different approach in [30], where no such assumptions on the source statistics are made. Comon and Moreau [9] find a closed-form solution for the maximization of a 4th-order contrast function earlier proposed in [18]. Other analytic expressions are found in [11, 12] from the maximization of output squared cumulant criteria. Though most of these methods are seemingly disparate, a closer examination shows that certain relationships exist among them.

1.5. Aim and Structure

Our aim is to provide a generic framework for the closed-form solutions to the BSS problem. Links between existing analytic procedures are revealed, new methods are proposed, and the performance of the techniques considered is analyzed. Drawbacks manifested by some of these methods are also highlighted, and are circumvented in some cases. We first address the real-valued mixture case; the companion paper [34] extends some of the present results to the complex-mixture case.

All solutions are identical for infinite sample size. However, their finite-sample performances, which are obtained in practice, are potentially different. Stressing these discrepancies is one of the key objectives of the present contribution. The statistics of practical datasets are

implicitly corrupted by some amount of "sampling noise", due to the finite sample length. Accordingly, the methods' performance in noisy environments would be expected to differ similarly as they do in noiseless finite-sample conditions.

The paper is structured as follows. In Section 2, we relate two equivalent analytical formulae suggested in [5, 8, 14] to the approximate ML (AML) solution of [10] and to the extended ML (EML) method of [30]. The first estimator is understood in finer detail. Later, in Section 3 a family of analytic estimators based on the nth-order cumulants is uncovered. Interestingly, the EML estimator is a particular case of such class, for $n = 4$. This new general class is considered from the perspective of optimization principles in Section 4. It is shown that each estimator of the family is the closed-form solution to an associated contrast function. At fourth-order, this result broadens the applicability domain of a contrast function proposed in [18]. Section 5 puts forward another 4th-order estimator which is aimed at alleviating a deficiency of the other 4th-order estimators considered in the prevous sections: the dependence of their performance on certain source statistic. The idea is to combine the different expressions through a decision rule, that we derive empirically. Illustrative computer experiments are reported in Section 6. To finalize the exposition, Section 7 summarizes the conclusions. The two appendices contain, respectively, the estimators' asymptotic analysis and the proofs of mathematical results established throughout the paper.

1.6. Nomenclature and Notational Conventions

The following mathematical and statistical terms will hold in the sequel. $\mathrm{E}[\cdot]$ denotes the mathematical expectation, whereas $\mathrm{Var}[\cdot]$ refers to the variance. $\mathrm{Cum}^z_{i_1\ldots i_n} \triangleq \mathrm{Cum}[z_{i_1}, \ldots, z_{i_n}]$ represents the nth-order cumulant of the components of real-valued random vector $\boldsymbol{z}$. For the two signal scenario this notation is simplified as $\mathrm{Cum}^z_{\underbrace{1\ldots1}_{n-r}\,\underbrace{2\ldots2}_{r}} = \kappa^z_{n-r,r}$, which is Kendall's convention for the two-dimensional case [22]. We call kurtosis of z_i its 4th-order marginal cumulant, Cum^z_{iiii}. Accordingly, in the two-dimensional case, κ^z_{40} and κ^z_{04} represent the kurtosis of components z_1 and z_2, respectively. The skewness corresponds to the 3rd-order marginal cumulant, $\kappa^z_{30} = \mathrm{Cum}^z_{111}$, $\kappa^z_{03} = \mathrm{Cum}^z_{222}$. Symbol $\mu^x_{mn} = \mathrm{E}[x_1^m x_2^n]$ stands for the $(m+n)$th-order moment of the source signals $\boldsymbol{x} = (x_1, x_2)$. Totally analogous terminology holds for the other random variables and vectors used in this paper. Symbols γ and η represent, respectively, the source kurtosis sum (sks) and source kurtosis difference (skd): $\gamma \triangleq \kappa^x_{40} + \kappa^x_{04}$, $\eta \triangleq \kappa^x_{40} - \kappa^x_{04}$.

Sets $\mathbb{N} \triangleq \{\ldots, -1, 0, 1, 2, \ldots\}$, $\mathbb{N}^+ \triangleq \{1, 2, \ldots\}$, $\mathbb{R}$ and $\mathbb{C}$ contain, respectively, the integer, positive integer, real and complex numbers. In addition, $\angle a$ stands for the principal value of the argument of $a \in \mathbb{C}$, and $(\cdot)^*$ for the complex-conjugation operator. The sample size is represented by T.

Finally, for the sake of clarity Table 1 defines the acronyms used in this paper.

2. Connections among Direct Methods

In the two-source two-sensor scenario of real signals and mixtures, matrix $\boldsymbol{Q}$ becomes an elementary Givens rotation of unknown angle θ:

$$\boldsymbol{Q} = \boldsymbol{\mathcal{Q}}(\theta)\,, \tag{4}$$

where

$$\boldsymbol{\mathcal{Q}}(\cdot) : \mathbb{R} \mapsto \mathbb{R}^{2\times 2}, \quad \boldsymbol{\mathcal{Q}}(\theta) = \begin{bmatrix} \cos\theta & -\sin\theta \\ \sin\theta & \cos\theta \end{bmatrix}. \tag{5}$$

Table 1. List of acronyms.

Acronym	Definition
ACF	alternative CF
AEML	alternative EML
AML	approximate maximum likelihood
BSS	blind source separation
CDMA	code division multiple access
CF	Comon's formula
combEML	combined EML
ECG	electrocardiogram
EEG	electroencephalogram
EML	extended maximum likelihood
FDMA	frequency division multiple access
HOEVD	higher-order eigenvalue decomposition
HOS	higher-order statistics
ICA	independent component analysis
i.i.d.	independent and identically distributed
ISR	interference-to-signal ratio
JADE	joint approximate diagonalization of eigenmatrices
MC	Monte Carlo
ML	maximum likelihood
MSE	mean squared error
MUD	multiuser detection
MUI	multiuser interference
PCA	principal component analysis
pdf	probability density function
PRBS	pseudorandom binary sequence
skd	source kurtosis difference
sks	source kurtosis sum
SOK	sum of output kurtosis
TDMA	time division multiple access
TOBSE	third-order blind signal estimator

Therefore, the separation is reduced to the estimation of a single relevant parameter, angle θ. The characteristics of this simplified scenario are restrictive, and rather of a theoretical nature. However, a clear understanding of the problem in this basic set-up is of primal importance, since the solution in more elaborate practical environments (such as more than two signals, noisy observations, etc.) may benefit from results on this fundamental case [7, 31]. For instance, the general scenario composed of more than two signals can be tackled through an iterative approach over the signal pairs [7].

Two equivalent estimation formulae which appear in [5], [8], and [14] are recalled in Section 2.1. Section 2.2 reviews, for the sake of completeness, two other 4th-order estimators. The connection is made in Section 2.3.

2.1. Two Equivalent Estimators

By nulling a 4th-order cross-cumulant of the signals at the separator output, a closed-form expression for the estimation of θ is found in [5]. This formula reads:

$$\operatorname{tg} \hat{\theta}_{\mathrm{CF}} = -\rho/2 + \operatorname{sign}(\rho)\sqrt{\rho^2/4 + 1}\,, \tag{6}$$

where

$$\rho \triangleq \frac{\kappa^z_{31} - \kappa^z_{13}}{\kappa^z_{22}}\,. \tag{7}$$

The acronym *CF* stands for *Comon's formula*. From Equations (2) and (4), the 4th-order cumulants of the whitened observations can be expanded as a function of the unknown angle θ and the 4th-order cumulants of the sources. The following are the expressions for the cross-cumulants:

$$\kappa^z_{31} = \cos^3\theta \sin\theta \kappa^x_{40} - \cos\theta \sin^3\theta \kappa^x_{04} \tag{8}$$

$$\kappa^z_{22} = \cos^2\theta \sin^2\theta (\kappa^x_{40} + \kappa^x_{04}) \tag{9}$$

$$\kappa^z_{13} = \cos\theta \sin^3\theta \kappa^x_{40} - \cos^3\theta \sin\theta \kappa^x_{04} \tag{10}$$

symbols κ^x_{40} and κ^x_{04} denoting the 4th-order marginal cumulants, or kurtosis, of the source signals. Now, using the above expressions and expanding the trigonometric functions results in [8, 14]:

$$\operatorname{tg}(2\hat{\theta}_{\mathrm{ACF}}) = \frac{2}{\rho}\,. \tag{11}$$

Resorting to the formula of the tangent of the double angle, it turns out that $\hat{\theta}_{\mathrm{CF}}$ and $\hat{\theta}_{\mathrm{ACF}}$ are simply the same estimates, even for finite sample size. On these grounds, Equation (11) may be referred to as *alternative Comon's formula (ACF)*. Although these two estimators are equivalent, the ACF will prove more useful when studying their performance (Section 2.3).

2.2. The AML and EML Estimators

The AML Estimator

Adopting the ML approach and using the Gram–Charlier expansion of the source probability density function (pdf), an estimator for the unknown parameter θ is found in [10]. When written as a function of the 4th-order cumulants of the whitened signals it reads:

$$\operatorname{tg}(4\hat{\theta}_{\mathrm{AML}}) = \frac{\mathrm{E}[r^4 \sin\phi]}{\mathrm{E}[r^4 \cos\phi]} = \frac{4(\kappa^z_{31} - \kappa^z_{13})}{\kappa^z_{40} - 6\kappa^z_{22} + \kappa^z_{04}}\,, \quad r\mathrm{e}^{j\phi} = z_1 + jz_2, \quad j = \sqrt{-1}. \tag{12}$$

In this development the sources are assumed to have the same symmetric distribution and normalized kurtosis in the interval [0, 4]. The latter restriction is imposed by the validity conditions of the Gram–Charlier expansion.

The EML Estimator
The EML estimator is based on the expressions [28, 30]:

$$\xi = (\kappa_{40}^z - 6\kappa_{22}^z + \kappa_{04}^z) + j4(\kappa_{31}^z - \kappa_{13}^z) = (\kappa_{04}^x + \kappa_{04}^x)e^{j4\theta} \tag{13}$$

$$\gamma = \kappa_{40}^z + 2\kappa_{22}^z + \kappa_{04}^z = \kappa_{40}^x + \kappa_{04}^x\,. \tag{14}$$

yielding:

$$\hat{\theta}_{\text{EML}} = \frac{1}{4}\angle(\xi \cdot \text{sign}(\gamma))\,. \tag{15}$$

Both ξ and γ admit a compact expression as a function of the whitened-signal scatter-plot points, like in (12):

$$\begin{cases} \xi = \text{E}[r^4 e^{j4\phi}] \\ \gamma = \text{E}[r^4] - 8\,. \end{cases} \tag{16}$$

Estimator (15) generalizes (12) in the sense that it can be used for any source distribution, as long as the source kurtosis sum γ is not null. The main asymptotic results of this estimator are summarized in Appendix A.1; a more comprehensive study is accomplished in [30]. A straightforward adaptive version is proposed and analyzed in [33].

2.3. Link and Discussion

Connection between AML and CF
Appropriate trigonometric transformations on (11) produce:

$$\text{tg}(4\hat{\theta}_{\text{ACF}}) = \frac{2\text{tg}(2\hat{\theta})}{1 - \text{tg}^2(2\hat{\theta})} = \frac{4\rho}{\rho^2 - 4} \tag{17}$$

which, with the relationship among the whitened 4th-order cumulants proved in [5], reduces to the AML estimator (12). However, for finite sample size the above mentioned cumulant relationship does not hold. Only CF (6) and ACF (11) are identical estimates even for finite sample size. For infinite sample length (and hence exact cumulant values) all methods provide, obviously, the same solution: the true value of the unknown parameter.

Connection between AML and EML
This link was established in [27, 28, 30]. We may write (12) as the argument (angle with respect the real axis) of ξ in (13), whereby it becomes patent that no meaningful estimation of θ can be achieved if $\kappa_{40}^x + \kappa_{04}^x = 0$. The AML manifests a $\pm 45°$ bias when the sks is negative. The estimator was originally developed under the assumption of sources with positive kurtosis, but it is only necessary that the sks be positive, which is a weaker assumption.

New AML Expression
AML can be made applicable to negative sks if the estimation is explicitly carried out as a function of parameter ρ, as in Equation (17). This is equivalent to dividing the real and imaginary parts of (13) by κ_{22}^z, which, according to (9), has always the same sign as the sks. That is, combining (9) and (13):

$$\frac{(\kappa_{40}^z - 6\kappa_{22}^z + \kappa_{04}^z)}{\kappa_{22}^z} + j\frac{4(\kappa_{31}^z - \kappa_{13}^z)}{\kappa_{22}^z} = (\rho^2 - 4) + j4\rho = (\cos\theta \sin\theta)^{-2}\text{e}^{j4\theta}. \tag{18}$$

CF Dependency on Unknown Parameter
According to the previous equation, the CF/ACF estimator (6)/(11) is, as the EML, valid for any sign of sks. However, the CF performance depends on the parameter θ. Effectively, the CF/ACF estimator can directly be written as

$$\hat{\theta}_{\text{ACF}} = \frac{1}{2}\angle\xi_{\text{ACF}}\,, \tag{19}$$

where the complex centroid ξ_{ACF} is given by

$$\xi_{\text{ACF}} = (\kappa_{31}^z - \kappa_{13}^z) + j2\kappa_{22}^z = \frac{1}{2}\gamma \sin 2\theta \mathrm{e}^{j2\theta}. \tag{20}$$

The phase shift introduced by the term $\gamma \sin 2\theta$ is not important: it would simply mean a $\pm\pi/2$ radian bias in θ, which does not affect the source separation. From this expression, the asymptotic variance of the CF estimator can easily be obtained (Appendix A.2), and can be formulated as:

$$\sigma_{\text{CF}}^2 = \sigma_{\text{EML}}^2 + \Delta\sigma^2(\theta)\,, \tag{21}$$

where function $\Delta\sigma^2(\theta)$ is given by the corresponding term in Equation (59), and symbols σ_{EML}^2 and σ_{CF}^2 represent the asymptotic variances of the EML and CF estimators, respectively. The CF performance is hence dependent on the unknown parameter θ, as opposed to the EML, which is orthogonal invariant [30]. We have that $\sigma_{\text{CF}}^2 \geq \sigma_{\text{EML}}^2$, $\forall\theta$, when there is a symmetric source or both sources have identical distribution (actually it is only required that they have equal 3rd- and 5th-order moments). Otherwise, values of θ could exist for which $\sigma_{\text{CF}}^2 < \sigma_{\text{EML}}^2$, and a non-symmetric performance with θ could be manifested by the CF. For θ close to zero the CF quality severely degrades in all cases, and a considerably higher variance than EML's is expected.

3. A Closed-Form Estimation Family

In this section, the 4th-order estimator (15) is found to be a particular case of a wider family of closed-form estimators. The following result establishes a connection between the nth-order cumulants of the whitened observations and those of the sources whereby the parameter of interest may be estimated at once.

THEOREM 1. *Define $\xi_n(\boldsymbol{z})$ as the following weighted sum of pairwise nth-order cumulants of the components of $\boldsymbol{z}$, with $n \in \mathbb{N}^+$:*

$$\xi_n(\boldsymbol{z}) \triangleq \sum_{r=0}^{n} \binom{n}{r} j^r \kappa_{n-r,r}^{\boldsymbol{z}}\,. \tag{22}$$

If $\boldsymbol{z} = \boldsymbol{\mathcal{Q}}(\theta)\boldsymbol{x}$, with $\boldsymbol{x}$ made up of independent components, then

$$\xi_n(\boldsymbol{z}) = \mathrm{e}^{jn\theta}\xi_n(\boldsymbol{x})\,, \tag{23}$$

where, according to (22), $\xi_n(\boldsymbol{x}) = \kappa_{n0}^{\boldsymbol{x}} + j^n\kappa_{0n}^{\boldsymbol{x}}$.

The statistic $\xi_n(\cdot)$ is termed *nth-order complex centroid*. The significance of the above result lies in the fact that, from (23), the hidden rotation can be estimated in analytic form as:

$$\hat{\theta}_n = \frac{1}{n}\angle\left(\frac{\xi_n(z)}{\xi_n(\boldsymbol{x})}\right). \tag{24}$$

In a genuine blind problem the source statistics, and hence $\xi_n(\boldsymbol{x})$, are unknown. But in some situations $\xi_n(\boldsymbol{x})$ can be estimated from the available data, as illustrated next. First, we observe that formula (24) must be applied with some care.

Solution Indeterminacy
As $n\theta = n(\theta + 2\pi m/n)$, for any $n, m \in \mathbb{N}$, it turns out that the actual angle value supplied by estimator (24) at order n can be any of the form $\hat{\theta}_n = \theta + 2\pi m/n$, $m \in \mathbb{N}$. The only order at which this solution indeterminacy is acceptable is, in principle, $n = 4$, since then the possible bias takes the form $\pm k\pi/2$, and this still recovers the source waveforms up to order permutation and unitary scale factors (permitted indeterminacies, as commented in Section 1). Accordingly, the indeterminacy is also admissible at second order, but we will see later that at $n = 2$ Equation (24) is not of use any more. At order $n = 3$, it will also be seen below than the indeterminacy can be resolved. At any order $n > 4$, there is no other option than considering together the set of possible solutions $\hat{\theta}_n + 2\pi k/n$, $k = 0, 1, \ldots, n-1$, and deciding by means of an extra criterion (such as degree of output statistical independence) which of those n values is correct.

Theorem 1 will be extended to the complex case in the companion paper [34]. Estimation scheme (24) is now studied at different orders.

Second Order
At order 2 we have:

$$\xi_2(z) = (\kappa_{20}^z - \kappa_{02}^z) + j2\kappa_{11}^z = \mathrm{e}^{j2\theta}(\kappa_{20}^x - \kappa_{02}^x) = 0\,, \tag{25}$$

owing to the source unit-variance convention. So no meaningful estimation can be carried out by (25) at this order. This was to be expected, since all second-order information is depleted after pre-whitening. Indeed, no second-order based technique is able to recover the missing orthogonal transformation if the temporal structure cannot be exploited (as in the i.i.d. case) or is just ignored [31]. At orders 3 and 4, the situation is quite different. We will see that in those cases estimator (24) can be used without the need for prior knowledge of the source statistics.

Third Order
In this case:

$$\xi_3(z) = (\kappa_{30}^z - 3\kappa_{12}^z) + j(3\kappa_{21}^z - \kappa_{03}^z) = \mathrm{e}^{j3\theta}(\kappa_{30}^x - j\kappa_{03}^x)\,. \tag{26}$$

In principle, we would need to know κ_{30}^x and κ_{03}^x in order to estimate θ through (26):

$$\hat{\theta}_3 = \frac{1}{3}\angle\left(\frac{\xi_3(z)}{\gamma_3}\right), \quad \gamma_3 \triangleq \kappa_{30}^x - j\kappa_{03}^x\,, \tag{27}$$

but then this estimator would still be suffering from the solution indeterminacy commented above. Nevertheless, a closer look at the 3rd-order cumulants of $\boldsymbol{z}$ – bearing in mind to multilinearity property of cumulants and the statistical independence of the components in $\boldsymbol{x}$ [1] – reveals that:

$$\kappa_{21}^z + j\kappa_{12}^z = \tfrac{1}{2}\sin 2\theta\,\mathrm{e}^{j\theta}(\kappa_{30}^x - j\kappa_{03}^x) = \gamma_3'\,. \tag{28}$$

Hence, substituting (28) into (26): $\xi_3(\boldsymbol{z})/\gamma_3' = \frac{2}{\sin 2\theta}\mathrm{e}^{j2\theta}$, and so θ may be estimated at order 3 via:

$$\hat{\theta}_3 = \frac{1}{2}\angle\left(\frac{\xi_3(\boldsymbol{z})}{\gamma_3'}\right), \tag{29}$$

selecting $\hat{\theta}_3 = 0$ if $\gamma_3' = 0$. This is called *Third-Order Blind Signal Estimator (TOBSE)*. The possible negative sign introduced by the term $\sin 2\theta$ of γ_3' is irrelevant, as it would result in a $\pm\pi/2$ radian bias in θ which does not affect the source recovery. Also, the solution indeterminacy is avoided, since the argument of $\xi_3(\boldsymbol{z})/\gamma_3'$ depends on twice the true angle θ. Naturally, this 3rd-order estimator is applicable as long as there is at least one asymmetric source. If this condition holds, it may be wiser to employ this 3rd-order estimator rather than a 4th-order one since, for the same number of samples, cumulant estimates are generally more accurate at lower orders. This notion will be endorsed by the experimental results in Section 6. Finally, remark that TOBSE statistics may also be computed from the whitened scatter-plot points in polar form, as for the AML (12) and EML (15) methods:

$$\xi_3(\boldsymbol{z}) = \mathrm{E}[(z_1 + jz_2)^3] = \mathrm{E}[r^3\mathrm{e}^{j3\phi}] \tag{30}$$

$$\gamma_3' = E[z_1 z_2(z_1 + jz_2)] = \mathrm{E}[\frac{1}{2}r^3\mathrm{e}^{j\theta}\sin 2\phi]\,. \tag{31}$$

A simplified asymptotic analysis of this estimator can be found in Appendix A.3.

Fourth Order
At $n = 4$ expression (23) develops into:

$$\xi_4(\boldsymbol{z}) = (\kappa_{40}^z - 6\kappa_{22}^z + \kappa_{04}^z) + j4(\kappa_{31}^z - \kappa_{13}^z) = \mathrm{e}^{j40}(\kappa_{40}^x + \kappa_{04}^x) = \mathrm{e}^{j4\theta}\gamma\,, \tag{32}$$

which is the EML centroid ξ (13). Again, we do not need to have any prior knowledge of the source distribution (provided $\gamma \neq 0$), since the sks may be estimated from the whitened signals as in Equations (14) and (16). As $\gamma \in \mathbb{R}$, only its sign is of interest for the estimation of θ.

4. Optimality Principles

The family of estimators defined by Equation (24) can be seen as resulting from the optimization of respective cumulant matching and contrast function criteria (Section 4.1). In particular, this will allow us to establish an interesting connection between the EML estimator and another contrast-based method encountered in the bibliography (Sections 4.2 and 4.3). Before unveiling such criteria, we first need the following corollary of Theorem 1.

COROLLARY 2. *Define the output vector as a counter-rotation of angle $\hat{\theta}$ performed on the whitened signal space, i.e., $\boldsymbol{s} = \boldsymbol{\mathcal{Q}}(-\hat{\theta})\boldsymbol{z}$. Then, with the relationships introduced in Theorem 1:*

$$\xi_n(\boldsymbol{s}) = \mathrm{e}^{-jn\hat{\theta}}\xi_n(\boldsymbol{z})\,. \tag{33}$$

4.1. General Optimization Criteria

THEOREM 3. *The family of estimators given analytically by Equation (24) are the local minimizers of*

$$J_{\mathrm{m}n}(\hat{\theta}) = |\xi_n(\boldsymbol{s}) - \xi_n(\boldsymbol{x})|^2 = |\xi_n(\boldsymbol{z})\mathrm{e}^{-jn\hat{\theta}} - \xi_n(\boldsymbol{x})|^2, \tag{34}$$

or, equivalently, the local maximizers of

$$J_{\mathrm{M}n}(\hat{\theta}) = \mathbb{R}\mathrm{e}(\xi_n(\boldsymbol{x})^*\xi_n(\boldsymbol{s})) = \mathbb{R}\mathrm{e}(\xi_n(\boldsymbol{x})^*\xi_n(\boldsymbol{z})\mathrm{e}^{-jn\hat{\theta}})\,. \tag{35}$$

Minimization of (34) corresponds to an nth-order cumulant matching criterion whereby the mismatch between a linear combination of output nth-order cumulants ($\xi_n(\boldsymbol{s})$) and the same linear combination of source cumulants ($\xi_n(\boldsymbol{x})$) is minimized. Maximization of (35) yields a contrast function optimization criterion. According to Theorem 3, the optimization of these equivalent criteria is solved in closed-form by (24).

4.2. Contrast Function at Fourth Order

At fourth order, Equation (35) corresponds to the contrast function of the EML estimator. This settles the question raised in [32] of whether an optimization criterion existed for this estimator. In turn, this also proves that the EML estimator is orthogonal invariant [2, 3], i.e., its performance does not depend on the particular value of $\boldsymbol{Q}$ (property which was already manifested when analyzing its performance in [30]). By virtue of (22), function (35) at $n = 4$ can be written as a function of the output cumulants:

$$J_{\mathrm{EML}} = J_{\mathrm{M4}} = \mathbb{R}\mathrm{e}(\xi_4(\boldsymbol{x})^*\xi_4(\boldsymbol{s})) = \gamma\,(\kappa_{40}^s - 6\kappa_{22}^s + \kappa_{04}^s)\,. \tag{36}$$

The significance of the following result will become apparent in the next section.

LEMMA 4. *The functions J_{EML} in Equation (36) and*

$$\tilde{J}_{\mathrm{EML}} = \varepsilon_\gamma(\kappa_{40}^s + \kappa_{04}^s), \quad \text{with } \varepsilon_\gamma \triangleq \mathrm{sign}(\gamma)\,, \tag{37}$$

have identical local extrema. In particular, the local maxima of $\tilde{J}_{\mathrm{EML}}$ are given in closed-form by (24), with $n = 4$.

4.3. Extension of Moreau's Contrast Function

A 4th-order contrast function is proposed in [18], which is valid when all the sources have the same kurtosis sign, say ε. In the two-signal case, this function reads:

$$I_4(\boldsymbol{s}) = \varepsilon(\kappa_{40}^s + \kappa_{04}^s), \quad \varepsilon \triangleq \mathrm{sign}(\kappa_{40}^x) = \mathrm{sign}(\kappa_{04}^x)\,. \tag{38}$$

A rather cumbersome analytical solution (that we call SOK, for "sum of output kurtosis") was given in [9] for the maximization of (38). However, if the sign of sks ε_γ is substituted for the sign of source kurtosis ε, Lemma 4 provies that: (a) the SOK solution gracefully reduces to the EML estimator; (b) by virtue of this simple modification I_4 is made applicable, under the EML conditions, to scenarios where the sources may show dissimilar tail (kurtosis sign); and (c) the need for the prior knowledge of the source tail is spared, since the sks can be estimated from the available information as in (14)/(16).

For more than two signals, the pairwise application of contrast $\tilde{J}_{\text{EML}}$ (37), i.e., of the EML analytic solution (15), provides satisfactory results in all experiments carried out by the authors. This is a somewhat surprising outcome, since it is not generally true that the multidimensional extension of $\tilde{J}_{\text{EML}}$ is a valid contrast.

5. An Alternative Fourth-Order Estimator

5.1. The Alternative EML

Fourth-order estimators CF, AML and EML lose their consistency when the sks is zero. To overcome this deficiency, and in the spirit of Section 3, we seek another complex linear combination of the whitened-signal 4th-order cumulants that supplies an explicit expression for the unknown parameter θ. Let us define:

$$\xi'_4(\boldsymbol{z}) \triangleq (\kappa^z_{40} - \kappa^z_{04}) + 2j\,(\kappa^z_{31} + \kappa^z_{13})\,. \tag{39}$$

Then:

$$\xi'_4(\boldsymbol{z}) = \mathrm{e}^{j2\theta}\xi'_4(\boldsymbol{x})\,, \tag{40}$$

where, according to (39), $\xi'_4(\boldsymbol{x}) = \eta$, since the source components are independent. Accordingly, the following estimator of θ can be used when the source kurtosis difference (skd) η is not null:

$$\hat{\theta}'_4 = \frac{1}{2}\angle\xi'_4(\boldsymbol{z}) = \hat{\theta}_{\text{AEML}}\,. \tag{41}$$

The estimation of η is not necessary, for it can only cause an immaterial $\pm\pi/2$ radian bias. Observe also that $\xi'_4(\boldsymbol{z})$ can compactly be computed as

$$\xi'_4(\boldsymbol{z}) = \mathrm{E}[(z_1^2 + z_2^2)((z_1^2 - z_2^2) + j2z_1z_2)] = \mathrm{E}[r^4\mathrm{e}^{j2\phi}]\,. \tag{42}$$

Due to its analogies with the EML, this estimator is called *alternative EML (AEML)*. Appendix A.4 provides its main asymptotic results [27].

Given a set of whitened signals, which estimator, EML or AEML, should be used? A sensible optimal choice would be to take the one with the smallest mean squared error (MSE). But the MSE depends in both cses on the source statistics [27], and in a blind problem these are unknown. We are left with adopting a suboptimal decision strategy based on the available information.

5.2. An Empirically-Based Suboptimal Decision Rule

In a bid to obtain a tractable practical guideline to decide between the 4th-order estimators EML and AEML, their performance is evaluated for different values of sks γ and skd η. This can be achieved by using pseudorandom binary sequences (PRBS) as sources [29]. Resorting to these ideas, κ^x_{40} is fixed at –2, whereas the kurtosis of the second source (κ^x_{04}) is varied between –2 and 14. Signal realization are composed of $T = 5 \cdot 10^3$ samples. At each kurtosis value separations are performed by the two methods on the same orthogonal mixtures of $\theta = 30°$, and a performance index is averaged over 100 independent Monte Carlo (MC) runs. The performance index must be selected with care. For instance, the estimated-angle MSE is

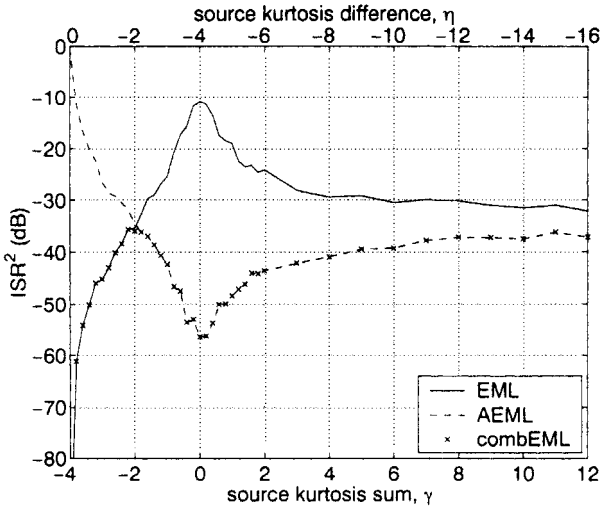

Figure 1. Performance of EML, AEML and combined estimators vs. sks and skd. PRBS sources, $\kappa_{40}^x = -2, \theta = 30°$.

not an effective measure, because several angle values provide equivalent separation solutions (all angles of the form $\theta + m\pi/2$, $m \in \mathbb{N}$). Instead, we compute the interference-to-signal ratio (ISR) [31], which quantifies the average interference caused by the unwanted sources in the recovery of the desired sources. In our set-up, it is defined as:

$$\mathrm{ISR} = \mathop{\mathrm{E}}_{i \neq j} \left\{ \frac{|(\widehat{\boldsymbol{Q}}^{\mathrm{T}} \boldsymbol{Q})_{ij}|^2}{|(\widehat{\boldsymbol{Q}}^{\mathrm{T}} \boldsymbol{Q})_{ii}|^2} \right\}, \tag{43}$$

where notation $(\boldsymbol{A})_{ij}$ represents the element (i, j) of matrix $\boldsymbol{A}$ (after rearranging its columns to place the dominant entries in its diagonal). Since $\hat{\boldsymbol{x}} = \boldsymbol{s} = \widehat{\boldsymbol{Q}}^{\mathrm{T}} \boldsymbol{Q}\boldsymbol{x} = \boldsymbol{\mathcal{Q}}(\theta - \hat{\theta})\boldsymbol{x}$ and the true sources are assumed unit-variance, the ISR becomes a good approximation of the estimated-angle variance when $\hat{\theta} \approx \theta + m\pi/2$, $m \in \mathbb{N}$, i.e., at valid separation solutions.

Figure 1 shows the results.[1] As expected, EML and AEML worsen around $\gamma = 0$ and $\eta = 0$, respectively. Taking into account that

$$\begin{aligned} |\xi_4(z)| &= |\kappa_{40}^x + \kappa_{04}^x| = |\gamma| \\ |\xi_4'(z)| &= |\kappa_{40}^x + \kappa_{04}^x| = |\eta| \end{aligned} \tag{44}$$

the performance of both methods deteriorates when their respective centroids are close to the origin of the complex plane. For $\gamma < -2$, the EML shows better performance than the AEML, and conversely when $\gamma > -2$. So an alternation in best performance occurs when the signs of source kurtosis pass from being equal (EML is better) to being different (AEML is better). These results lead to the following decision rule between the two methods:

$$\kappa_{40}^x \kappa_{04}^x \underset{\text{AEML}}{\overset{\text{EML}}{\gtrless}} 0\,. \tag{45}$$

[1] For a clearer comparison, the mean square value of ISR has been plotted in dB, where $\mathrm{ISR}^2(\mathrm{dB}) = 5\log_{10}(\mathrm{E}[\mathrm{ISR}^2])$. The justification for "5" lies in the fact that ISR is already a quadratic quantity [Equation (43)]. Therefore, when using this measure both location (bias) and dispersion (variance) information about ISR are condensed in the results.

Straightforward algebraic manipulations transform the above expression into:

$$(\kappa_{40}^x + \kappa_{04}^x)^2 \underset{\text{AEML}}{\overset{\text{EML}}{\gtrless}} (\kappa_{40}^x - \kappa_{04}^x)^2 \,. \tag{46}$$

Bearing in mind Equations (44), this is turned into a practical decision rule, i.e., a principle that can be applied from the available information, which reads:

$$|\xi_4(z)| \underset{\text{AEML}}{\overset{\text{EML}}{\gtrless}} |\xi_4'(z)| \,. \tag{47}$$

Thus, if the modulus of the EML centroid (13) is bigger than the modulus of the AEML centroid (39), then the former should be applied, and conversely. Intuitively, this empirical rule of thumb makes sense: choose the estimator with the largest centroid modulus. The hybrid estimation scheme derived from (47) is referred to as *combined EML (combEML)*. As shown in Figure 1, the combEML consistently maintains the best performance over all range of sks and skd. Additional experiments on continuous distributions corroborate decision rule (47) [27].

6. Simulation Results

A number of simulations endorse and illustrate the theoretical exposition of the previous sections. In what follows all signals are composed by 5000 samples, and MC iterations are run over 100 independent mixture realizations. For a given simulation, identical signal realizations are fed into all methods considered. Performance measure ISR (see Section 5.2) is averaged over all these iterations, and is the value represented at each point in the plots.

The first experiment demonstrates the dependence of CF estimator on parameter θ. Figure 2 shows the results obtained with the CF (6), the AML (12) and the EML (15) for orthogonal rotations of different angles on source signals with an exponential and a uniform distribution. As seen in Section 2.3, the CF estimator performance varies with θ, whereas the other two do not. Note also that, since the sks is positive, AML provides identical performance as EML, even though the experimental set-up contradicts the original assumptions of [10] (different source distributions, an asymmetric source with kurtosis outside validity of Gram–Charlier expansion). This is in accordance with the exposition in Section 2.3, [28] and [30].

Testing the accuracy of the asymptotic results is the main objective of the second simulation. Figure 3 shows the performance variation of the EML (15), CF (6) and TOBSE (29) estimators, together with their respective expected asymptotic variances, Equations (56), (59) and (61), as a function of the unknown angular parameter θ. The source pdfs chosen are exponential (long-tailed, asymmetric) and asymmetric triangular (short-tailed). CF performance follows very accurately the theoretically anticipated asymmetric trend, with a severe deterioration around $\theta = m\pi/2$ rad, $m \in \mathbb{N}$ (Section 2.3). The EML, which shows a flat response with θ, improves the CF across the whole angle range besides very small regions around –30° and 60°. TOBSE also exhibits an asymmetric variation with θ for these source distributions. A performance degradation similar to that of the CF is also observed near the "critical" regions $\theta = m\pi/2$ rad, $m \in \mathbb{N}$. As a result, the fitness of its analytic variance is precise only outside the cited areas. Further investigations are required to overcome these unforeseen practical

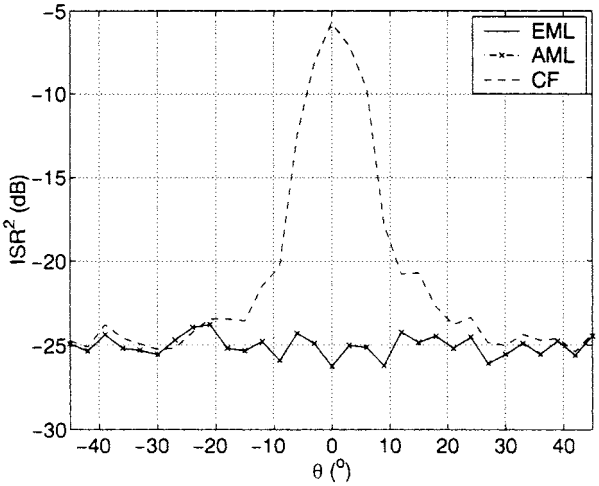

Figure 2. Mean square ISR vs. angular parameter θ. Exponential and uniform source distributions.

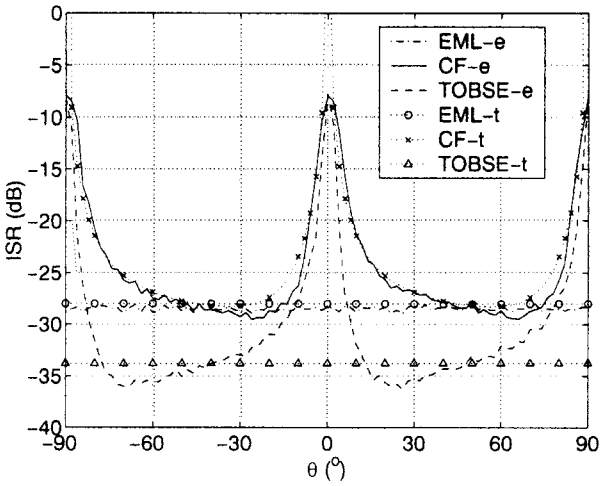

Figure 3. Performance of the EML, CF and TOBSE estimators vs. angle θ. Exponential and asymmetric triangular sources, 500 MC runs. Legend suffixes: "e", empirical; "t", theoretical.

limitations, which are probably introduced by the term γ_3' [Equation (28)] in the estimator expression. However, TOBSE improves, by up to 10 dB, the 4th-order methods over most angle range.

The third experiment compares several closed-form solutions studied in this paper, and is run along the lines of the simulation described in Section 5.2. Now the combined estimator (15) and (41) together with decision rule (47) is tested along the EML, AML and CF, setting $\theta = 10°$. Figure 4 shows that the EML consistently provides better performance than the CF and the AML. The latter is biased for negative sks. The use of the combined strategy avoids the performance worsening around zero sks and improves it for positive sks. TOBSE is also considered. As the sks varies between –4 and 12, the skewness of one of the sources varies between 0 and –4 [29]. TOBSE performance appears nearly independent of the source skewness values, and improves the 4th-order estimators EML, AML, and CF over most values

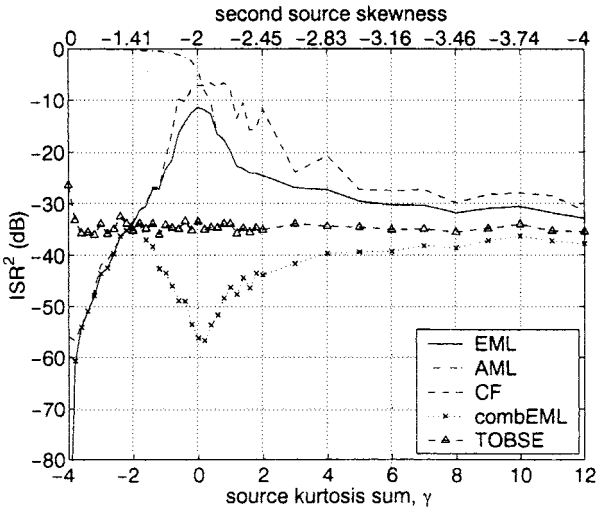

Figure 4. Mean square ISR vs. sks and source skewness. PRBS sources, $\kappa_{40}^{x} = -2, \theta = 10°$.

of sks/source skewness. As pointed out in Section 3, the higher estimation accuracy of 3rd-order cumulants relative to 4th-order ones may account for this outcome.

The purpose of the final experiment is to contrast the EML with SOK, to illustrate the results of Section 4.3, and to make a comparison to other well-established BSS methods. ICA-HOEVD (higher-order eigenvalue decomposition) [7] and JADE (joint approximate diagonalization of eigenmatrices) [4]. The ICA-HOEVD is based on contrast function optimization, specifically, on maximizing the sum of output squared kurtosis, whereas JADE relies on the joint diagonalization of particular cumulant-tensor matrix slices. The method labelled as SOK′ corresponds to the direct solution SOK, but using the sign of sks ε_γ as estimated by (14) instead of the kurtosis sign of both sources. Here, for the SOK the source kurtosis is assumed to be always positive, $\varepsilon = 1$. Results of Figure 5 confirm that, effectively, SOK′ solutions coincide with the EML estimates. In fact, even SOK coincides with EML when the sks is positive, although the sources themselves have different kurtosis sign. Hence, the use of contrast (38) can indeed be extended as commented in Section 4.2. It is interesting to observe how the combEML outperforms ICA-HOEVD and JADE by about 4 dB in this simulation. Also remark the identical trend exhibited by their respective curves, and the deterministic performance [3, Section VII-C] of these three methods for equiprobable-symbol PRBS sources ($\gamma = -4$). Effectively, $\sigma^2_{\text{EML}} = 0$ for symmetric binary sources. In contrast, observe that the AEML can never enjoy deterministic performance.

7. Summary, Conclusions and Outlook

MUD in multiuser wireless communications can be formulated as a BSS problem. This contribution has addressed a number of issues related to closed-form estimators for the blind separation of instantaneous linear mixtures. In the first place, the connections among CF, AML and EML have been established. The AML could not be used for negative sks but, thanks to the link evidenced, an equivalent expression for this estimator has been found overcoming this deficiency. The CF performance has been shown to depend on the unknown angular parameter.

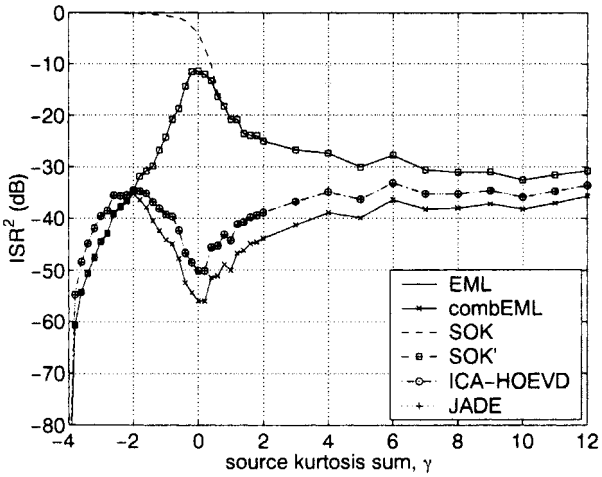

Figure 5. Mean square ISR vs. sks. PRBS sources, $\kappa_{40}^{x} = -2, \theta = 10°$.

Therefore, the EML estimator emerges as the best option among those three methods: it is valid for any sign of sks and its performance is independent of the unknown parameter.

In the second place, a general family of estimators based on the higher-order statistics has been determined. It is based on specific complex liner combinations of the whitened-signal cumulants which preserve explicit expressions for the unknown parameter. At 4th-order, this general class yields the EML method. Also, a new 3rd-order estimator, so-called TOBSE, has been derived from the family. It can be applied when at least one of the sources is asymmetric, and in most of the experiments it has offered better performance than its 4th-order counterparts; this outcome may be due to the lower estimation error of 3rd-order cumulants.

Contrast-function/cumulant-matching optimization criteria have been associated with the closed-form estimation family. This result has proven specially fruitful in the fourth-order case, for the applicability of a known contrast function has been expanded and the EML has been found to be its analytical solution.

The EML performance deterioration for near-zero sks has been solved by putting forward another 4th-order estimator, the AEML. A heuristic decision rule has been derived to select between the two expressions given a batch of whitened observations. The resultant combined estimation strategy exhibits a performance variation with the source 4th-order statistics similar to well-established contrast-based BSS methods such as JADE and ICA-HOEVD.

Several matters deserve further investigation. As a first point, some type of phase unwrapping strategy could be developed in order to surmount the indeterminacy problem of estimation family (24), thereby allowing direct estimation at any order greater than four. Whether this strategy would actually be beneficial should also be a subject of careful consideration, since the estimation errors at high orders could render any effort in that direction useless. An approach to the multi-signal case different from the iterative pairwise technique [7] could be devised by looking into combinations of cumulants involving more than two components. How the noise influences the estimation performance needs to be looked into as well.

This paper has provided the first unified vision of analytic estimators for BSS. Hence, it is hoped by the authors that this work will open fresh new avenues of research on the topic.

References

1. D.R. Brillinger, *Time Series. Data Analysis and Theory*, Holden-Day Inc.: San Francisco, CA, 1981.
2. J.F. Cardoso, "On the Performance of Orthogonal Source Separation Algorithms", in *Proceedings EUSIPCO*, Edingburgh, U.K., 1994, pp. 776–779.
3. J.F. Cardoso, "Blind Signal Separation: Statistical Principles", *Proceedings of the IEEE*, Vol. 86, No. 10, pp. 2009–2025, 1998.
4. J.-F. Cardoso and A. Souloumiac, "Blind Beamforming for Non-Gaussian Signals", *IEE Proceedings-F*, Vol. 140, No. 6, pp. 362–370.
5. P. Comon, "Separation of Stochastic Processes", in *Proceedings Workshop on Higher-Order Spectral Analysis*, Vail, CO, 1989, pp. 174–179.
6. P. Comon, "Higher-Order Separation, Application to Detection and Localization", in *Proceedings EUSIPCO*, Barcelona, Spain, 1990, pp. 277–280.
7. P. Comon, "Independent Component Analysis, A New Concept?", *Signal Processing*, Vol. 36, No. 3, pp. 287–314.
8. P. Comon and P. Chevalier, "Blind Source Separation: Models, Concepts, Algorithms and Performance", in S.S. Haykin (ed.), *Unsupervised Adaptive Filtering, Vol. I: Blind Source Separation*, Wiley Series in Adaptive and Learning Systems for Communications, Signal Processing and Control, John Wiley & Sons: New York, 2000.
9. P. Comon and E. Moreau, "Improved Contrast Dedicated to Blind Separation in Communications", in *Proceedings ICASSP*, Munich, Germany, 1997, pp. 3453–3456.
10. F. Harroy and J.-L. Lacoume, "Maximum Likelihood Estimators and Cramer-Rao Bounds in Source Separation", *Signal Processing*, **55**, pp. 167–177, 1996.
11. F. Herrmann and A.K. Nandi, "Maximisation of Squared Cumulants for Blind Source Separation", *IEE Electronics Letters*, Vol. 36, No. 19, pp. 1664–1665.
12. F. Herrmann and A.K. Nandi, "Blind Separation of Linear Instantaneous Mixtures Using Closed-Form Estimators", *Signal Processing*, Vol. 81, pp. 1537–1556, 2001.
13. T.-P. Jung, S. Makeig, T.-W. Lee, M.J. McKeown, G. Brown, A.J. Bell and T.J. Sejnowski, "Independent Component Analysis of Biomedical Signals", in *Proceedings 2nd Int. Workshop on Independent Component Analysis and Signal Separation*, Helsinki, Finland, 2000, pp. 633–644.
14. J.-L. Lacoume, P.-O. Amblard and P. Comon, *Statistiques d'Ordre Supérieur pour le Traitement du Signal*, Collection Sciences de l'Ingénieur, Masson: Paris, 1997.
15. J.-L. Lacoume and P. Ruiz, "Separation of Independent Sources from Correlated Inputs", *IEEE Transactions on Signal Processing*, Vol. 40, No. 12, pp. 3074–3078, 1992.
16. L.D. Lathauwer, D. Callaerts, B.D. Moor and J. Vandewalle, "Fetal Electrocardiogram Extraction by Source Subspace Separation", in *Proceedings IEEE/ATHOS Signal Processing Conference on Higher-Order Statistics*, Girona, Spain, 1995, pp. 134–138.
17. S. Makeig, A.J. Bell, T.-P. Jung and T.J. Sejnowski, "Independent Component Analysis of Electroencephalographic Data", *Advances in Neural Information Processing Systems*, Vol. 8, pp. 145–151, 1996.
18. E. Moreau, "Criteria for Complex Source Separation", in *Proceedings EUSIPCO*, Trieste, Italy, 1996, pp. 931–934.
19. T. Ojanperä and R. Prasad, *Wideband CDMA for Third Generation Mobile Communications*, Artech House: Boston, MA, 1998.
20. J.J. Rieta, V. Zarzoso, J. Millet-Roig, R. García-Civera and R. Ruiz-Granell, "Atrial Activity Extraction Based on Blind Source Separation as an Alternative to QRST Cancellation for Atrial Fibrillation Analysis", in *Computers in Cardiology*, Boston, MA, 2000, pp. 67–72.
21. R.J. Serfling, *Approximation Theorems of Mathematical Statistics*, Wiley Series in Probability and Mathematical Statistics, John Wiley & Sons: New York, 1980.
22. A. Stuart and J.K. Ord, *Kendall's Advanced Theory of Statistics, Vol. I*, Edward Arnold: London, sixth edition, 1994.
23. N. Thirion, J. Mars and J.-L. Boelle, "Separation of Seismic Signals: A New Concept Based on a Blind Algorithm", in *Proceedngs EUSIPCO*, Trieste, Italy, 1996, pp. 85–88.
24. K. Torkkola, "Blind Separation for Audio Signals – Are We There Yet?", in *Proceedings 1st International Workshop on Independent Component Analysis and Signal Separation*, Assois, France, 1999, pp. 239–244.
25. M.K. Tsatsanis and D. Slock, "Multi-User Communications/Multi-User Detection", in G. Giannakis (ed.), "Highlights of Signal Processing for Communications", *IEEE Signal Processing Magazine*, pp. 38–42, 1999.

26. S. Verdú, *Multiuser Detection*, Cambridge University Press: Cambridge, U.K., 1998.
27. V. Zarzoso, "Closed-Form Higher-Order Estimators for Blind Separation of Independent Source Signals in Instantaneous Linear Mixtures", Ph.D. Thesis, The University of Liverpool, U.K., 1999.
28. V. Zarzoso and A.K. Nandi, "Generalization of a Maximum-Likelihood Approach to Blind Source Separation", in *Proceedings EUSIPCO*, Vol. IV, Rhodes, Greece, 1998a, pp. 2069–2072.
29. V. Zarzoso and A.K. Nandi, "Modelling Signals of Arbitrary Kurtosis for Testing BSS Methods", *IEE Electronics Letters*, Vol. 34, No. 1, pp. 29–30, 1998b. (Errata: Vol. 34, No. 7, Apr. 2, p. 703, 1998).
30. V. Zarzoso and A.K. Nandi, "Blind Separation of Independent Sources for Virtually Any Source Probability Density Function", *IEEE Transactions on Signal Processing*, Vol. 47, No. 9, pp. 2419–2432, 1999a.
31. V. Zarzoso and A.K. Nandi, "Blind Source Separation", in A.K. Nandi (ed.), *Blind Estimation Using Higher-Order Statistics*, Kluwer Academic Publishers: Boston, MA, pp. 167–252, 1999b.
32. V. Zarzoso and A.K. Nandi, "Blind Source Separation without Optimization Criteria?", in *Proceedings ICASSP*, Vol. III, Phoenix, AZ, 1999c, pp. 1453–1456.
33. V. Zarzoso and A.K. Nandi, "Adaptive Blind Source Separation for Virtually Any Source Probability Density Function", *IEEE Transactions on Signal Processing*, Vol. 48, No. 2, pp. 477–488, 2000.
34. V. Zarzoso and A.K. Nandi, "Noninvasive Fetal Electrocardiogram Extraction: Blind Separation Versus Adaptive Noise Cancellation", *IEEE Transactions on Biomedical Engineering*, Vol. 48, No. 1, pp. 12–18, 2001b.
35. V. Zarzoso and A.K. Nandi, "Closed-Form Estimators for Blind Separation of Sources – Part II: Complex Mixtures", *Wireless Personal Communications*, Vol. 21, No. 1, pp. 29–48, 2002.

Appendix A. Asymptotic Performance Analysis

This appendix summarizes the large-sample performance results of the estimators studied in this paper. The general result is as follows. Let an angle estimate $\hat{\theta}$ be obtained from a sample estimate of a whitened-observation complex centroid $\hat{\xi}$ via

$$\hat{\theta} = \frac{1}{r}\angle\hat{\xi}\,. \tag{48}$$

Also, assume that $\hat{\xi}$ accepts the formulation

$$\hat{\xi} = \Delta\hat{\xi}\mathrm{e}^{jr\theta}, \quad \text{with } \Delta\hat{\xi} = |\Delta\hat{\xi}|\mathrm{e}^{j\delta} \tag{49}$$

denoting the sample estimate of the associated source centroid. Then, the error of estimate $\hat{\theta}$ is

$$\Delta\hat{\theta} \triangleq (\hat{\theta} - \theta) = \delta/r\,. \tag{50}$$

Now, given the complex variable

$$\Delta\hat{\xi} = \omega_1 + j\omega_2 = \frac{1}{T}\sum_{k=1}^{T}(\tilde{\omega}_1(k) + j\tilde{\omega}_2(k))\,, \tag{51}$$

such that $\tilde{\omega}_1(k)$ and $\tilde{\omega}_2(k)$ are functions of the i.i.d. random vector $\boldsymbol{x}(k)$, and

$$\begin{aligned} m &= \mathrm{E}[\omega_1] = \mathrm{E}[\tilde{\omega}_1], \quad \mathrm{E}[\omega_2] = \mathrm{E}[\tilde{\omega}_2] = 0, \\ \sigma_2^2 &= \mathrm{Var}[\omega_2] = \frac{1}{T}\mathrm{Var}[\tilde{\omega}_2] \end{aligned} \tag{52}$$

then the asymptotic (as $T \to \infty$) pdf of $\delta = \angle\Delta\hat{\xi}$ is proven to be [27]:

$$p_\delta(\delta) \underset{T\to\infty}{\approx} \hat{p}_\delta(\delta) = \frac{1}{\sqrt{2\pi}\sigma_2/|m|}\exp\left\{\frac{-\delta^2}{2(\sigma_2/m)^2}\right\}\,. \tag{53}$$

Therefore, from this last result and Equation (50), the estimation error is asymptotically distributed as

$$\Delta\hat{\theta} \xrightarrow[T\to\infty]{\mathrm{d}} \mathrm{N}(0, \sigma_2^2/(rm)^2)\,, \tag{54}$$

in which $\xrightarrow{\mathrm{d}}$ indicates convergence in distribution [21]. Alternatively, identical asymptotic results are obtained from the small-error analysis of the associated contrast function [27].

A.1. EML Estimator

For the EML estimator (15) we have [30]:

$$\begin{aligned} \Delta\hat{\xi} &= \frac{1}{T}\sum_{k=1}^{T}(x_1(k) + jx_2(k))^4 \\ m &= \gamma \\ \sigma_2^2 &= 16(\mu_{60}^x + \mu_{06}^x - 2\mu_{40}^x\mu_{04}^x)/T\,, \end{aligned} \tag{55}$$

providing the asymptotic variance:

$$\sigma_{\mathrm{EML}}^2 = \frac{\mu_{60}^x + \mu_{06}^x - 2\mu_{40}^x\mu_{04}^x}{T\gamma^2}\,. \tag{56}$$

The EML is asymptotically unbiased (unbiased for any sample size if one of the sources is symmetric) and strongly consistent as long as $\gamma \neq 0$ [30].

A.2. CF Estimator

In the case of the CF/ACF estimator (19), one obtains:

$$\Delta\hat{\xi} = \frac{1}{4jT}\sum_{k=1}^{T}\{(x_1(k) + jx_2(k))^4\mathrm{e}^{j2\theta} - [(x_1^2(k) + x_2^2(k))^2 - 8]\mathrm{e}^{-j2\theta}\}$$

$$m = \frac{1}{2}\gamma\sin 2\theta \tag{57}$$

$$\begin{aligned} \sigma_2^2 \;=\; & [4(\mu_{40}^x\mu_{04}^x - 1)\cos^2 2\theta + (\mu_{60}^x + \mu_{06}^x - 2\mu_{40}^x\mu_{04}^x)\sin^2 2\theta \\ & + 4(\mu_{50}^x\mu_{03}^x - \mu_{30}^x\mu_{05}^x)\cos 2\theta \sin 2\theta]/T\,. \end{aligned} \tag{58}$$

These parameters yield the large-sample variance:

$$\sigma_{\mathrm{CF}}^2 = \sigma_{\mathrm{EML}}^2 + \frac{4}{T\gamma^2\mathrm{tg}2\theta}\left\{\frac{(\mu_{40}^x\mu_{04}^x - 1)}{\mathrm{tg}2\theta} + (\mu_{50}^x\mu_{03}^x - \mu_{30}^x\mu_{05}^x)\right\}\,. \tag{59}$$

The CF is asymptotically unbiased and strongly consistent provided $m \neq 0$, that is, as long as both the sks γ and angle θ are not null. The dependency of σ_{CF}^2 on θ only vanishes for two symmetric binary sources, in which case the CF, like the EML, presents deterministic performance ($\sigma^2 = 0$).

A.3. TOBSE Estimator

Due to the term γ_3' in expression (29), the study of TOBSE asymptotic performance is more complicated than for the 4th-order methods. An approximate analysis can be carried out by considering non-blind estimator (27) instead, providing an optimistic or "best-case" bound of performance.

Estimator (27) can alternatively be written as $\hat{\theta}_3 = \frac{1}{3}\angle\hat{\xi}_3'$, with $\hat{\xi}_3' = \hat{\xi}_3\gamma_3^*$. This results in:

$$\begin{aligned}
&\Delta\hat{\xi} = \frac{\gamma_3^*}{T}\sum_{k=1}^{T}(x_1(k) + jx_2(k))^3 \\
&m = |\gamma_3|^2 \\
&\sigma_2^2 = [(\kappa_{30}^x)^2(\mu_{06}^x + 9\mu_{40}^x - 6\mu_{04}^x) + (\kappa_{03}^x)^2(\mu_{60}^x + 9\mu_{04}^x - 6\mu_{40}^x) \\
&\qquad - 20(\kappa_{30}^x\kappa_{03}^x)^2]/T\,,
\end{aligned} \tag{60}$$

and an asymptotic variance:

$$\sigma_{\text{TOBSE}}^2 \approx \frac{\sigma_2^2}{9|\gamma_3|^4}\,. \tag{61}$$

A.4. AEML Estimator

For the AEML estimator (41):

$$\begin{aligned}
&\Delta\hat{\xi} = \frac{1}{T}\sum_{k=1}^{T}(x_1^2(k) + x_2^2(k))(x_1(k) + jx_2(k))^2 \\
&m = \eta \\
&\sigma_2^2 = 4(\mu_{60}^x + \mu_{06}^x + 2\mu_{40}^x\mu_{04}^x)/T\,,
\end{aligned} \tag{62}$$

resulting in

$$\sigma_{\text{AEML}}^2 = \frac{\mu_{60}^x + \mu_{06}^x + 2\mu_{40}^x\mu_{04}^x}{T\eta^2}\,. \tag{63}$$

Provided the skd η is finite, the estimator is asymptotically unbiased and strongly consistent.

Appendix B. Proofs

B.1. Proof of Theorem 1

Due to the multilinearity property of cumulants and the statistical independence of the components in $\boldsymbol{x}$ [1], we can write:

$$\kappa_{n-r,r}^z = \sum_{i_1\cdots i_n} q_{1i_1}\cdots q_{1i_{n-r}}q_{2i_{n-r+1}}\cdots q_{2i_n}\text{Cum}_{i_1\cdots i_n}^x = q_{11}^{n-r}q_{21}^r\kappa_{n0}^x + q_{12}^{n-r}q_{22}^r\kappa_{0n}^x\,, \tag{64}$$

where $q_{ij} = (\boldsymbol{Q})_{ij}$ are the entries of the orthogonal transformation. Substituting this expression into (22) and noting that $q_{11} = q_{22} = \cos\theta$, $q_{21} = -q_{12} = \sin\theta$, we obtain:

$$\begin{aligned}\xi_n(z) &= \sum_{r=0}^{n} \binom{n}{r} j^r [(\cos\theta)^{n-r}(\sin\theta)^r \kappa_{n0}^x + (-\sin\theta)^{n-r}(\cos\theta)^r \kappa_{0n}^x] = \\ &= \kappa_{n0}^x \sum_{r=0}^{n} \binom{n}{r} (\cos\theta)^{n-r}(j\sin\theta)^r + j^n \kappa_{0n}^x \sum_{r=0}^{n} \binom{n}{r} (j\sin\theta)^{n-r}(\cos\theta)^r ,\end{aligned} \tag{65}$$

where, to go from the second to the third term, we have made use of the relations $j^r = j^n j^{-(n-r)} = j^n (j^{-1})^{n-r} = j^n (-j)^{n-r}$. Now, in order to simplify the summatories, we resort to Newton's binomial expansion:

$$\begin{aligned}\sum_{r=0}^{n} \binom{n}{r} (\cos\theta)^r (j\sin\theta)^{n-r} &= \sum_{r=0}^{n} \binom{n}{r} (\cos\theta)^{n-r}(j\sin\theta)^r = \\ &= (\cos\theta + j\sin\theta)^n = \mathrm{e}^{jn\theta}.\end{aligned} \tag{66}$$

So, finally:

$$\xi_n(z) = \mathrm{e}^{jn\theta}(\kappa_{n0}^x + j^n \kappa_{0n}^x) = \mathrm{e}^{jn\theta}\xi_n(\boldsymbol{x}) . \tag{67}$$

The last equality is due to the source independence, which makes all source cross-cumulants vanish.

B.2. Proof of Corollary 2

$\boldsymbol{s} = \boldsymbol{\mathcal{Q}}(-\hat{\theta})\boldsymbol{z} = \boldsymbol{\mathcal{Q}}(-\hat{\theta})\boldsymbol{\mathcal{Q}}(\theta)\boldsymbol{x} = \boldsymbol{\mathcal{Q}}(\theta - \hat{\theta})\boldsymbol{x}$, so, by successive application of Theorem 1: $\xi_n(\boldsymbol{s}) = \mathrm{e}^{jn(\theta-\hat{\theta})}\xi_n(\boldsymbol{x}) = \mathrm{e}^{-jn\hat{\theta}}(\mathrm{e}^{jn\theta}\xi_n(\boldsymbol{x})) = \mathrm{e}^{-jn\hat{\theta}}\xi_n(\boldsymbol{z})$.

B.3. Proof of Theorem 3

Since $J_{\mathrm{m}n}(\hat{\theta}) = (\xi_n(\boldsymbol{z})\mathrm{e}^{-jn\hat{\theta}} - \xi_n(\boldsymbol{x}))(\xi_n(\boldsymbol{z})\mathrm{e}^{-jn\hat{\theta}} - \xi_n(\boldsymbol{x}))^* = |\xi_n(\boldsymbol{z})|^2 + |\xi_n(\boldsymbol{x})|^2 - 2\mathbb{R}\mathrm{e}(\xi_n(\boldsymbol{x})^*\xi_n(\boldsymbol{z})\mathrm{e}^{-jn\hat{\theta}}) = 2|\xi_n(\boldsymbol{x})|^2 - 2J_{\mathrm{M}n}(\hat{\theta})$, and $|\xi_n(\boldsymbol{x})|^2$ is constant for a given pair of sources, the minimization of $J_{\mathrm{m}n}$ is tantamount to the maximization of $J_{\mathrm{M}n}$. Thus, we only need to show the second part of the theorem.

The first and second derivatives of $J_{\mathrm{M}n}$ are, respectively:

$$\begin{aligned}\frac{\partial J_{\mathrm{M}n}}{\partial\hat{\theta}} &= n\mathbb{I}\mathrm{m}(\xi_n(\boldsymbol{x})^*\xi_n(\boldsymbol{z})\mathrm{e}^{-jn\hat{\theta}}) \\ \frac{\partial^2 J_{\mathrm{M}n}}{\partial\hat{\theta}^2} &= -n^2\mathbb{R}\mathrm{e}(\xi_n(\boldsymbol{x})^*\xi_n(\boldsymbol{z})\mathrm{e}^{-jn\hat{\theta}}) = -n^2 J_{\mathrm{M}n} .\end{aligned} \tag{68}$$

The local extrema of $J_{\mathrm{M}n}$ are hence given by the first-order necessary condition:

$$\frac{\partial J_{\mathrm{M}n}}{\partial\hat{\theta}} = 0 \Leftrightarrow \mathrm{e}^{j[\angle(\xi_n(\boldsymbol{x})^*\xi_n(\boldsymbol{z}))-n\hat{\theta}]} = \pm 1 . \tag{69}$$

The local maxima must fulfil, in addition, the second-order necessary condition $\frac{\partial J_{\mathrm{M}n}}{\partial\hat{\theta}} < 0$, which occurs if and only if $\mathrm{e}^{j[\angle(\xi_n(\boldsymbol{x})^*\xi_n(\boldsymbol{z}))-n\hat{\theta}]} = 1$. Hence $\hat{\theta}_{\mathrm{opt}} = \frac{1}{n}\angle(\xi_n(\boldsymbol{x})^*\xi_n(\boldsymbol{z})) + \frac{2\pi m}{n}$, $m \in \mathbb{N}$, which transforms into $\hat{\theta}_n$ with $\xi_n(\boldsymbol{x})^{-1} = \xi_n(\boldsymbol{x})^*/|\xi_n(\boldsymbol{x})|^2$.

B.4. Proof of Lemma 4

Due to the relationship between the outputs and the whitened signals, $\boldsymbol{s} = \boldsymbol{\mathcal{Q}}(-\hat{\theta})\boldsymbol{z}$, it turns out that $\frac{\partial s_1}{\partial \hat{\theta}} = s_2$ and $\frac{\partial s_2}{\partial \hat{\theta}} = -s_1$. By using these equations when differentiating the cumulants, we arrive at $J'_{\mathrm{EML}} = 16\gamma(\kappa^s_{31} - \kappa^s_{13})$. Similarly: $\tilde{J}'_{\mathrm{EML}} = 4\varepsilon_\gamma(\kappa^s_{31} - \kappa^s_{13})$. Hence: $J'_{\mathrm{EML}} = 4|\gamma|\tilde{J}'_{\mathrm{EML}}$. Both functions are proportional from the first derivative onwards, and thus have identical critical points.

Vicente Zarzoso was born in Valencia, Spain, on September 12, 1973. He attended the Universidad Politécnica de Valencia for the first four years of his degree, and the University of Strathclyde, Glasgow, U.K., on an Erasmus exchange programme for the final year his degree. In July 1996, he received the M.Eng. degree with the highest distinction (Premio Extraordinario de Terminación de Estudios) in telecommunications engineering from the Universidad Politécnica de Valencia. He was awarded a scholarship by the University of Strathclyde to study in the Signal Processing Division of the Department of Electronic and Electrical Engineering towards his Ph.D. degree, the first year of which was also partly funded by a grant from the Defence Evaluation and Research Agency (DERA) of the U.K. He received the Ph.D. degree from the Department of Electrical Engineering and Electronics. The University of Liverpool, Liverpool, U.K. in October 1999.

Since March 1999, he has been with the Signal Processing and Communications Group, Department of Electrical Engineering and Electronics, The University of Liverpool, Liverpool, U.K. He holds a Post-doctoral Research Fellowship awarded by the Royal Academy of Engineering, Westminster, London, U.K. His research interests include blind signal separation, higher-order statistics, statistical signal and array processing, and their application to communications and biomedical problems.

Asoke K. Nandi received the degree of Ph.D. from the University of Cambridge (Trinity College), U.K., in 1979. He held a scholarship at Trinity College during his doctoral studies at the Cavendish Laboratory, Cambridge. Since then he held several research positions: associateship in Rutherford Appleton Laboratory, Oxfordshire, U.K., and in the European Organization for Nuclear Research (CERN), Geneva, Switzerland, as well as Advanced Fellowship in the Department of Physics, Queen Mary College, London, U.K., and in the Department of Nuclear Physics, University of Oxford, U.K. In 1987, he joined the Imperial College, London, U.K., as the Solartron Lecturer in the Signal Processing Section of the Electrical Engineering Department. In 1991, he joined the Signal Processing Division of the Electronic and Electrical Engineering Department in the University of Strathclyde, Glasgow, U.K., as a Senior Lecturer; subsequently, he was appointed a Reader in 1995 and a Professor in 1998. In March 1999, he moved to the University of Liverpool, U.K., to take up the appointment to the David Jardine Chair of Electrical Engineering in the Department of Electrical Engineering and Electronics.

In 1983 he was part of the UAI team at CERN that discovered the three fundamental particles known as W^+, W^- and Z^0 providing the evidence for the unification of the electromagnetic and weak forces, which was recognized by the Nobel committee for Physics in 1984. Currently he is the head of the signal processing and communications research group, which includes a number of tenured academics and a group of doctoral and postdoctoral researchers with interests in the areas of nonlinear systems, non-Gaussian signal processing, and communications research. With his group he has been carrying out research in machine condition monitoring, signal modelling, system identification, communication signal processing, time delay estimation, biomedical signals, underwater sonar, application of artificial neural networks, ultrasonics, blind source separation, and blind deconvolution. Professor Nandi was awarded the Mountbatten Premium, Division Award of the Electronics and Communications Division, of the Institution of Electrical Engineers of the U.K. in 1998 and the Water Arbitration Prize of the Institution of Mechanical Engineers of the U.K. in 1999.

Professor Nandi has authored or coauthored over 200 technical publications including two books – titled *Automatic Modulation Recognition of Communication Signals* (1996) and *Blind Estimation Using Higher-Order Statistics* (1999) – and over 100 journal papers. He is a Fellow of the Cambridge Philosophical Society, the Institution of Electrical Engineers, the Institute of Mathematics and its Applications, and the Institute of Physics. Also, he is a Senior Member of the Institute of Electrical and Electronic Engineers as well as a Member of the British Computer Society and the European Association for Signal Processing.